J Plant Res (2013) 126:113–119
DOI 10.1007/s10265-012-0496-4

REGULAR PAPER

Microtubule stability affects the unique motility of F-actin in *Marchantia polymorpha*

Atsuko Era · Natsumaro Kutsuna · Takumi Higaki · Seiichiro Hasezawa · Akihiko Nakano · Takashi Ueda

Received: 27 November 2011 / Accepted: 20 April 2012 / Published online: 8 June 2012

Abstract Actin microfilaments play crucial roles in diverse plant functions. Some specific cellular processes require interaction between F-actin and microtubules, and it is believed that there are direct or indirect connections between F-actin and microtubules. We previously reported that actin microfilaments exhibit unique dynamic motility in cells of the liverwort, *Marchantia polymorpha*; the relevance of this activity to microtubules has not been explored. To examine whether the dynamics of F-actin in *M. polymorpha* were somehow regulated by microtubules, we investigated the effects of stabilization or destabilization of microtubules on dynamics of actin bundles, which were visualized by Lifeact-Venus. To our surprise, both stabilization and destabilization of microtubules exerted similar effects on F-actin motility; apparent sliding movement of F-actin in *M. polymorpha* cells was accelerated by both oryzalin and paclitaxel, with the effect of paclitaxel more evident than that of oryzalin. Immunofluorescence staining revealed that some F-actin bundles were arrayed along with microtubules in *M. polymorpha* thallus cells. These results suggest that microtubules play regulatory roles in the unique F-actin dynamics in *M. polymorpha*.

Keywords Actin · Image analysis · Lifeact · *Marchantia polymorpha* · Microtubule

Electronic supplementary material The online version of this article (doi:10.1007/s10265-012-0496-4) contains supplementary material, which is available to authorized users.

A. Era · A. Nakano · T. Ueda (✉)
Department of Biological Sciences, Graduate School of Science, The University of Tokyo, Bunkyo-ku, Tokyo 113-0033, Japan
e-mail: tueda@biol.s.u-tokyo.ac.jp

N. Kutsuna · T. Higaki · S. Hasezawa
Department of Integrated Biosciences, Graduate School of Frontier Sciences, The University of Tokyo, 5-1-5 Kashiwanoha, Kashiwa, Chiba 277-8562, Japan

T. Higaki · S. Hasezawa
Advanced Measurement and Analysis, Japan Science and Technology Agency (JST), Chiyoda-ku, Tokyo 102-0076, Japan

A. Nakano
Molecular Membrane Biology Laboratory, RIKEN Advanced Science Institute, Wako, Saitama 351-0198, Japan

T. Ueda
Japan Science and Technology Agency (JST), PRESTO, 4-1-8 Honcho, Kawaguchi, Saitama 332-0012, Japan

Introduction

In plants, actin filaments (AFs) play fundamental roles in multiple cellular processes, including cytoplasmic streaming, organelle movement, cell morphogenesis, cell division, and tip growth (Hasezawa and Kumagai 2002; Hussey et al. 2006; Ketelaar and Emons 2001). Microtubules (MTs) are also important for plant cell morphogenesis, in both aspects of cell division and cell elongation (Baskin 2001; Granger and Cyr 2000; Van Damme et al. 2004). AFs and MTs are frequently observed concurrently in the same cellular structures. For example, during cell division they colocalize at the preprophase band, mitotic spindle, and phragmoplast with slightly different patterns (Collings and Allen 2000; Hoshino et al. 2003; Staiger and Cande 1991). The results of studies using actin filament-disrupting drugs suggest that AFs affect the arrangement of MTs (Eleftheriou and Palevitz 1992; Mineyuki and Palevitz 1990; Seagull 1990), and it has been also shown that MTs are required for correct reorganization of actin cables (Tominaga et al. 1997). These results indicate the existence

of direct and/or indirect interaction between these two cytoskeletal components in plant cells (Collings 2008). Several plant proteins have recently been identified that physically interact with both AFs and MTs (Collings 2008; Petrásek and Schwarzerová 2009). One such protein, *Arabidopsis thaliana* FORMIN14 (AFH14), reportedly acts as a linking protein between microtubules and actin filaments, a role that is critical for normal progression of cell division (Li et al. 2010). This evidence strongly suggests that linkage between AFs and MTs is critical to fulfill the functions of these cytoskeletons; however, our knowledge on its mechanism and physiological significance is still limited.

Lifeact, a marker that consists of the N-terminal 17 amino acids of yeast Abp140p, was recently successfully applied to various organisms as a new probe for visualizing AFs in living cells (Berepiki et al. 2010; Era et al. 2009; Riedl et al. 2008; Vidali et al. 2009). Using Lifeact, we visualized AFs in the liverwort, *Marchantia polymorpha*, and found them to be highly dynamic (Era et al. 2009). Directional sliding movement is one of the most distinctive features of AFs in *M. polymorpha*. However, the mechanism of this peculiar characteristic remains completely unknown.

In this study, we examined whether MTs play regulatory roles in the dynamic movement of AFs visualized with Lifeact-Venus in *M. polymorpha* cells, by treating thallus cells with microtubule-stabilizing or -depolymerizing drugs. We further examined the arrangement of AFs and MTs in *M. polymorpha* cells by immunofluorescent staining. These experiments provided interesting and novel information on the regulatory roles of MTs in the unique and dynamic sliding movement of AFs in *M. polymorpha*.

Materials and methods

Plant materials

Marchantia polymorpha was asexually propagated through gemma growth, as previously described (Okada et al. 2000; Takenaka et al. 2000). The transgenic *M. polymorpha* expressing Lifeact-Venus under the control of the Cauliflower mosaic virus 35S promoter was also described previously (Era et al. 2009).

Drug treatments

Young thalli with a longest diameter of approximately 5 mm were treated with 10 μM oryzalin, 10 μM paclitaxel, or 30 mM 2,3-butanedione-2-monoxime (BDM; Wako) for 2 h at room temperature. Oryzalin and paclitaxel were dissolved in dimethyl sulfoxide (DMSO) at 10 mM for stock solution, which were diluted with water for treating thalli. BDM was dissolved at 1 M in DMSO for stock solution, and diluted with water to the final concentration. For mock treatment, samples were treated with water containing DMSO at equal concentration to the inhibitor-treated samples.

Microscopy

For the observation of AFs visualized with Lifeact-Venus in *M. polymorpha*, thallus cells were observed under a fluorescent microscope (model BX51; Olympus, Tokyo, Japan) equipped with a confocal scanner unit (model CSU10, Yokogawa Electric, Tokyo, Japan) and cooled CCD camera (model ORCA-AG or ORCA-ER, Hamamatsu Photonics, Hamamatsu, Japan). Images were processed with the IPLab software (BD Biosciences, Rockville, MD, USA) and projection images were constructed using ImageJ software (http://rsb.info.nih.gov/ij/).

For double immunofluorescent staining of AFs and MTs in *M. polymorpha* cells, young wild-type thalli were treated with MBS solution (PMEG plus 250 μM *m*-maleimidobenzoyl-*N*-hydroxysuccinimide ester and 0.5 % Triton X-100) and then fixed with 3.7 % (w/v) formaldehyde in PMEG buffer (50 mM PIPES, 1 mM $MgSO_4$, 5 mM EGTA, and 1 % (v/v) glycerol, pH 6.8) for 1 h. Samples were washed three times with PMEG buffer and then incubated in an enzyme cocktail [PMEG plus 1 % cellulase Y-C (Kyowa), 0.05 % pectolyase Y-23 (Kyowa), 0.4 M mannitol, 5 mM EGTA, and a defined amount of protease inhibitor cocktail (Roche)] for 5 min. After washing three times with PMEG buffer, samples were treated with a detergent solution (PBS plus 1 % Nonidet P-40, 0.4 M mannitol, 5 mM EGTA, and a defined amount of protease inhibitor cocktail) for 15 min, washed three times with PBS, and blocked with glycine solution (PBS plus 0.1 M glycine, 1 % BSA, and 0.05 % Triton X-100) for 10 min. After washing three times with PBS, the thalli were incubated for 30 min with anti-α-tubulin antibody (Sigma-Aldrich) diluted in PBS (1:500), washed with PBS three times, and incubated in PBS-diluted (1:500) Alexa Fluor 488-conjugated goat anti-rat IgG (Molecular Probes) for 30 min. The samples were then washed with PBS three times and incubated with 165 nM Alexa Fluor 568-phalloidin in PBS. Double-stained samples were washed with PBS three times, mounted on a glass slide in PBS plus 0.1 % *p*-phenylenediamine, and observed under a confocal microscope (model LSM710, Carl Zeiss, Jena, Germany).

Image processing for evaluation of the movement index of F-actin

Workflow of the image processing is shown in Supplementary Fig. S1. To evaluate the movement index of the

AFs, we first obtained the subtracted images between time frame (t) and time frame ($t-1$) in the original time-sequential images (Fig. S1a, b). The subtracted image D visualizes the appeared and disappeared AFs as high and low intensity, respectively (Fig. S1b). It is defined by

$$D(\vec{p},t) = O(\vec{p},t) - O(\vec{p},t-1)$$

where O is an original time-sequential image, $\vec{p}$ is a coordinate of pixel, and t is an index of time frame.

To reduce the effect of the lateral fluctuation on the measurement of the AFs sliding activities, the subtracted images were filtered by our original shift-diffuse filter, which searches and obscures the fluctuated AFs (Fig. S1c). Based on the shift-diffuse filtered images and Otsu's thresholding algorithm (Otsu 1979), the regions of newly appeared AFs are determined (Fig. S1d). The thresholded image M is defined by

$$M(\vec{p},t) = \begin{cases} 1 & if\ D'\left(\vec{p} + \underset{\vec{s}\in Ps}{\arg\min}\left|D'(\vec{p},t) + D'\left(\vec{p}+\vec{S},t\right)\right|,t\right) > Thr \\ 0; & elsewhere \end{cases}$$

where D' is smoothed image of D with disc-shaped averaging kernel, Ps is an arbitrary point in the circle with a radius s (3 pixels in this study), and Thr is a threshold value determined by Otsu's method (Otsu 1979).

Then the image U visualizes the newly appeared AF segments, and is defined by

$$U(\vec{p},t) = T(\vec{p},t) \cdot M(\vec{p},t)$$

where T is AF-segmented image generated by KbiLineExtract (Fig. S1e) (Ueda et al. 2010). Finally, we calculated V_{AFs} as a movement index of AFs as follows:

$$V_{AFs} = \frac{\sum_{n=1}^{N_{seg}} L_n}{N_{seg}}$$

where L_n is length of n-th AF segment and N_{seg} is the number of AF segments in the image U. All image processing and calculations were performed using ImageJ software. The ImageJ macro used in this study is available at http://hasezawa.ib.k.u-tokyo.ac.jp/zp/Kbi/SkelSlide/.

Results

Effects of stabilization and destabilization of MTs

We previously introduced Lifeact-Venus into *M. polymorpha* to visualize AFs (Era et al. 2009), and found that actin cables in the young thallus cells moved dynamically (Fig. 1a; Era et al. 2009). In addition to lateral swinging movement, which has been observed in other plant cells (Higaki et al. 2006; Sheahan et al. 2004), we also observed actin cables sliding rapidly. In the present study, to examine whether MTs are somehow involved in the sliding movement of actin cables, we investigated the effects of stabilization and destabilization of MTs using paclitaxel and oryzalin, respectively. Figure 1 shows three time-sequential images of actin filaments in thallus cells taken at 3-s intervals, which have been colored red, green, or blue, and projected together. In the projected images, sliding actin cables are shown as colorful lines with gradation along a long axis of cables from red to blue (Fig. 1a, b, and Supplementary Movie S1). In contrast, immobile cables are shown as white lines, as observed in the projected images of actin cables treated with BDM, an inhibitor of myosin ATPase that inhibits movement of actin bundles in *M. polymorpha* cells (Fig. 1c and Supplementary Movie S2 (Era et al. 2009; Funaki et al. 2004; Tominaga et al. 2000). In contrast to our prediction that MTs might be required for actin cable sliding, treatment with oryzalin or paclitaxel did not restrain the movement of actin cables (Fig. 1d, e, and Supplementary Movies S3 and S4). Moreover, sliding velocity of actin cables seemed to be even faster in paclitaxel-treated cells than observed in the DMSO-treated control (Fig. 1e). We confirmed that the condition of oryzalin treatment employed here is sufficient for destruction of MTs in young thallus cells by immunofluorescent staining (Supplementary Fig. S2). Thus, MTs are not required for sliding movement of actin cables in *M. polymorpha* cells.

Quantitative analysis of movement of actin bundles

As mentioned above, paclitaxel treatment apparently accelerated the sliding of actin cables. For more quantitative evaluation of the drug effects, we developed an image analysis framework that automatically calculates the measurement that evaluates the movement activities of actin bundles from time-sequential images. 30 images of actin bundles taken every second were binarized, from which subtracted images between two sequential images were obtained, and then the length of remaining lines was measured for apparent length of migration. To reduce the effect of the lateral shift of actin bundles, we applied our original shift-diffuse filter (see "Materials and methods" and Supplementary Fig. 1 for detail of each step of the framework). We designated the value calculated by this framework as the "movement index". It should be noted that the moving index reflects apparent sliding velocity, because this framework does not distinguish newly polymerized filaments at the end of preexisting actin cables from sliding actin bundles. We quantified the movement index in each cell in control DMSO-treated ($n = 13$ cells), BDM-treated ($n = 9$), oryzalin-treated ($n = 17$), and

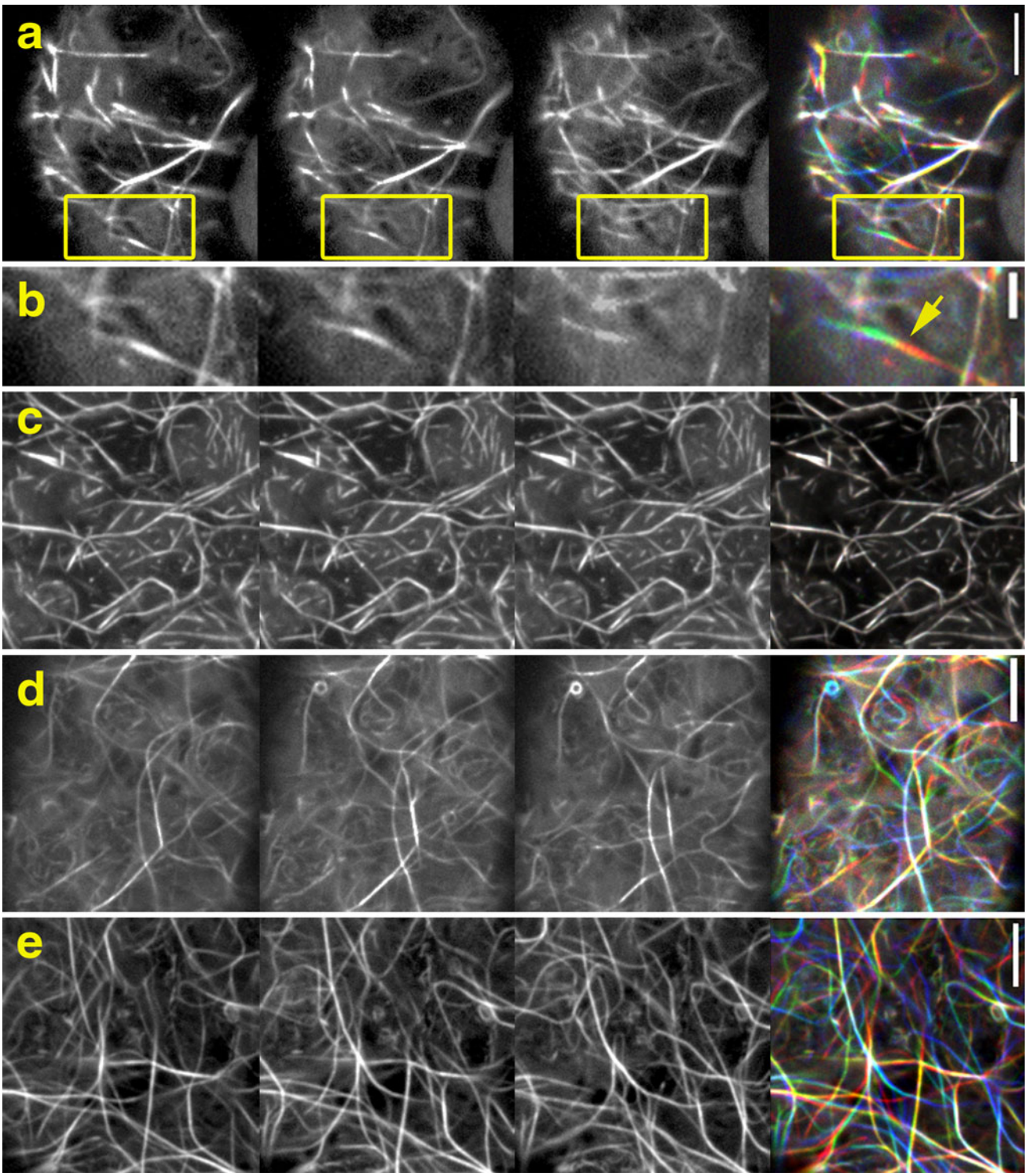

Fig. 1 Effects of drugs on dynamics of actin cables in *M. polymorpha* cells. Three serial images of actin filaments in thallus cells were taken at 0, 3, and 6 s (*left three columns*); their projections with each image colored *red*, *green*, or *blue* are presented in the right column. **a** Control, **b** magnified images of areas *squared* by *yellow boxes* in (**a**). The *arrow* shows a sliding actin cable. BDM-treated (**c**), oryzalin-treated (**d**), and paclitaxel-treated (**e**) thallus cells. *Scale bars* 5 μm (**a**, **c**–**e**) or 2 μm (**b**)

paclitaxel-treated ($n = 11$) thalli (Fig. 2). This quantification method detected significant inhibition of actin cable movement following BDM treatment [one-way ANOVA ($P < 0.01$) followed by Tukey–Kramer's post hoc test, $P < 0.05$] (Fig. 1c). This result indicated that this quantitative analysis could be efficiently used to detect the effect

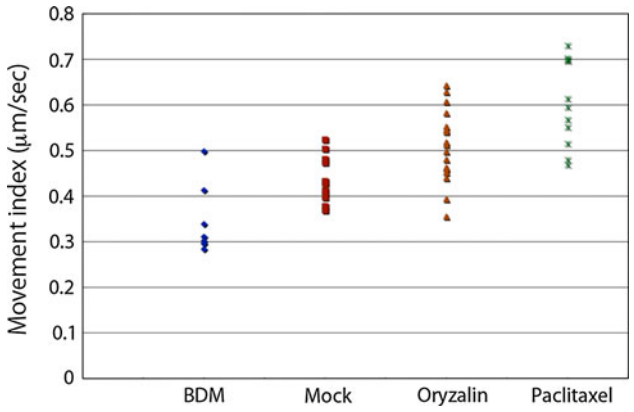

Fig. 2 Quantification of effects of drugs on movement of actin cables. The points are mean of movement indexes of actin cables in each cell treated with DMSO (control), BDM, oryzalin, or paclitaxel. $n = 9$–17

of each drug on the movement of actin cables. It should be noted that mean of movement indexes of all actin bundles in BDM-treated cells were much slower than 0.3 μm/s, because immobile segments were excluded from the calculation for V_{AFs} in this framework (Supplementary Fig. S1).

As we expected, the quantification method detected a significant accelerating effect of the paclitaxel treatment on actin cable movement (Tukey–Kramer's test, $P < 0.05$). Surprisingly, oryzalin treatment was also shown to confer the similar effect; the movement index was higher in oryzalin-treated cells than in control cells (Tukey–Kramer's test, $P < 0.05$). The accelerating speed of paclitaxel was significantly stronger than that of oryzalin (Tukey–Kramer's test, $P < 0.05$). These results indicated that both stabilization and destabilization of MTs confer similar effects on movement of actin cables in *M. polymorpha* cells.

Actin bundles and MTs in *M. polymorpha* cells

The results of drug treatments shown above indicated that MTs play some regulatory roles in dynamic movement of actin bundles, which suggests that these cytoskeletons interact with each other in non-dividing thallus cells of *M. polymorpha*. To verify this possibility, we carried out dual staining of endogenous AFs and MTs. MTs in young thallus cells were immunostained with anti-α-tubulin antibody and Alexa Fluor 488-conjugated goat anti-rat IgG. AFs were visualized with Alexa Fluor 568-phalloidin. As shown in Fig. 3, networks of actin bundles and MTs with various thicknesses were observed in these samples. Their overall patterns did not seem to overlap. However, close observation revealed that some of actin bundles and MTs were colocalized or closely co-aligned. We also observed some actin bundles bending along the adjacent MT bundles (boxes in Fig. 3a–d) or crossing between two MT bundles (arrows in Fig. 3a–c). This localization pattern might represent interaction between AFs and MTs at specific sites of the cytoskeletal network.

Discussion

Previous studies have revealed that AFs and MTs are arranged in a coordinated manner (Collings and Allen 2000), and that AF disruption resulted in changes of MT arrangement in various plant tissues (Eleftheriou and Palevitz 1992; Mineyuki and Palevitz 1990; Seagull 1990; Staiger and Cande 1991). In root hair cells of *Hydrocharis dubia*, it has been also shown that normal MT arrangement is required for reconstruction of actin cable networks after removal of cytochalasin B (Tominaga et al. 1997). These results strongly suggest the existence of direct and/or indirect interactions between AFs and MTs. Indeed, several plant proteins that interact with both of these cytoskeletons have been identified (Petrásek and Schwarzerová 2009). Thus it is plausible that motility and dynamics of AFs in the liverwort *M. polymorpha* are changed depending on the states of MTs; however, this has never been experimentally demonstrated thus far.

Dynamic directional sliding movement in addition to lateral swinging motion is a striking characteristic of actin cables in *M. polymorpha* (Era et al. 2009). We initially predicted that the interaction between MTs and AFs could be required for the sliding movement of actin bundles. Therefore, we examined the effect of a microtubule-depolymerizing drug (oryzalin) on this sliding movement, which would impede the actin bundle movement if our prediction was correct. However, oryzalin treatment did not hamper the sliding movement. Moreover, the quantitative analysis of actin bundle movement using our newly developed framework revealed that both depolymerization and stabilization of MTs exerted similar effects on the apparent sliding movement of actin bundles in *M. polymorpha*; AFs were more dynamic in both oryzalin- and paclitaxel-treated cells. These results indicated that in their normal state, MTs restrain the sliding movement of AFs, which is not the simple physical interference by MTs because both oryzalin and paclitaxel treatment accelerated the motility of actin bundles.

It is possible that the constraint that MTs exert on the sliding movement of actin bundles is mediated by other proteins that create physical or functional interactions between AFs and MTs. Candidates include *Arabidopsis thaliana* Formin4 (AFH4), which binds to MTs as well as acts in F-actin nucleation (Deeks et al. 2010). Other proteins, including SB401 (Huang et al. 2007; Liu et al. 2009)

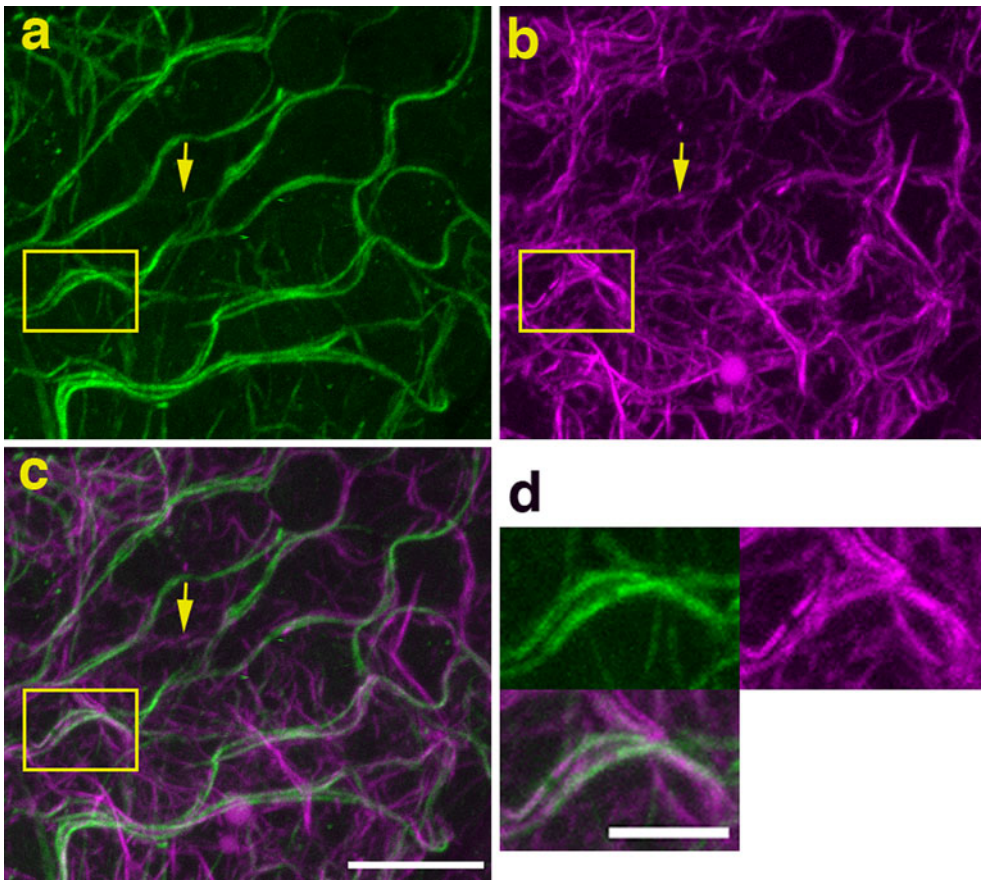

Fig. 3 Maximum intensity projection images of double-stained MTs (**a**) and actin filaments (**b**) in a thallus epidermal cell, reconstructed from a stack of 23 confocal images taken along the z-axis at 0.4 μm intervals. **c** The merged image of **a** and **b**. *Arrows* point to sites where actin bundles cross between two MT bundles. *Scale bar* 5 μm. **d** Magnified images of areas *squared* by *yellow boxes* in **a**, **b**, and **c**. *Scale bar* 2 μm

and AFH14 (Li et al. 2010), reportedly function in the bundling of both MTs and AFs. In this study, we showed by double immunostaining that some AF populations seemed to be tightly associated with MTs. Proteins such as AFH4, AFH14, and SB401,might link AFs and MTs in *M. polymorpha* cells, which could hinder the sliding movement of actin bundles. Our result that the MT-stabilizing drug paclitaxel and the MT-depolymerizing drug oryzalin conferred similar effects on the movement of actin bundles would be consistent with this notion. Hyper-stabilization of MTs might change the binding affinity between MTs and linker proteins, which could result in reduced physical hindrance of sliding movement of actin bundles.

As mentioned above, we demonstrated that MTs are not required for sliding movement of actin bundles. Our results also indicated that MTs do not act as a track for the sliding of AFs. Then, what are other candidates that determine the direction of the sliding movement of AFs in *M. polymorpha* cells? One possible candidate could be myosin. Myosin molecules arranged along organelle membranes or aligned on the plasma membrane might cause sliding movement of actin bundles, as in the case of the gliding assay in which F-actin slides on coverslips coated with myosin molecules. It would be an interesting future project to identify and localize *M. polymorpha* myosins to verify this possibility. In this case, MTs attached to the organelle membranes could also affect the sliding of actin bundles. Several plant kinesin molecules interact with both MTs and AFs (Frey et al. 2009; Preuss et al. 2004; Xu et al. 2009), and it is possible that myosin and kinesin interact with each other directly or indirectly, as proposed by Petrásek and Schwarzerová (2009). Our observations might reflect the inhibitory effect of such motor interactions on actin bundle sliding in *M. polymorpha* cells.

Because the dynamic sliding movement of actin bundles is unique to *M. polymorpha* cells, it is likely that unique molecular machineries for cytoskeletal dynamics exist in this organism. Future comparative analyses between *M. polymorpha* and other lineages of plants might unveil how the cytoskeleton system has diversified and evolved among land plant lineages.

Acknowledgments We would like to thank T. Kohchi and K. Ishizaki (Kyoto University), and K.T. Yamato (Kinki University) for

their generous support for *M. polymorpha* studies. This work was supported by Grants-in-Aid for Scientific Research and the Targeted Proteins Research Program (TPRP) from the Ministry of Education, Culture, Sports, Science, and Technology of Japan, and Grant-in-Aid for JSPS Fellows (A.E.). This research was also supported by JST, PRESTO.

References

Baskin TI (2001) On the alignment of cellulose microfibrils by cortical microtubules: a review and a model. Protoplasma 215:150–171

Berepiki A, Lichius A, Shoji JY, Tilsner J, Read ND (2010) F-actin dynamics in *Neurospora crassa*. Eukaryot Cell 9:547–557

Collings DA (2008) Crossed-wires: interaction and cross-talk between the microtubule and microfilament networks in plants. In: Nick P (ed) Plant microtubules, development and flexibility. Springer, Berlin, pp 47–82

Collings DA, Allen NS (2000) Cortical actin interacts with the plasme membrane and microtubules. In: Staiger CJ, Balusla F, Volkmann D, Barlow P (eds) Actin: a dynamic framework for multiple plant cell functions. Academic Publishers, Dordrecht, pp 145–163

Deeks MJ, Fendrych M, Smertenko A, Bell KS, Oparka K, Cvrcková F, Zarsky V, Hussey PJ (2010) The plant formin AtFH4 interacts with both actin and microtubules, and contains a newly identified microtubule-binding domain. J Cell Sci 123:1209–1215

Eleftheriou EP, Palevitz BA (1992) The effect of cytochalasin D on preprophase band organization in root tip cells of *Allium*. J Cell Sci 103:989–998

Era A, Tominaga M, Ebine K, Awai C, Saito C, Ishizaki K, Yamato KT, Kohchi T, Nakano A, Ueda T (2009) Application of lifeact reveals F-actin dynamics in *Arabidopsis thaliana* and the liverwort, *Marchantia polymorpha*. Plant Cell Physiol 50:1041–1048

Frey N, Klotz J, Nick P (2009) Dynamic bridges—a calponin-domain kinesin from rice links actin filaments and microtubules in both cycling and non-cycling cells. Plant Cell Physiol 50:1493–1506

Funaki K, Nagata A, Akimoto Y, Shimada K, Ito K, Yamamoto K (2004) The motility of *Chara corallina* myosin was inhibited reversibly by 2,3-butanedione monoxime (BDM). Plant Cell Physiol 45:1342–1345

Granger CL, Cyr RJ (2000) Microtubule reorganization in tobacco BY-2 cells stably expressing GFP-MBD. Planta 210:502–509

Hasezawa S, Kumagai F (2002) Dynamic changes and the role of the cytoskeleton during the cell cycle in higher plant cells. Int Rev Cytol 214:161–191

Higaki T, Kutsuna N, Okubo E, Sano T, Hasezawa S (2006) Actin microfilaments regulate vacuolar structures and dynamics: dual observation of actin microfilaments and vacuolar membrane in living tobacco BY-2 Cells. Plant Cell Physiol 47:839–852

Hoshino H, Yoneda A, Kumagai F, Hasezawa S (2003) Roles of actin-depleted zone and preprophase band in determining the division site of higher-plant cells, a tobacco BY-2 cell line expressing GFP-tubulin. Protoplasma 222:157–165

Huang S, Jin L, Du J, Li H, Zhao Q, Ou G, Ao G, Yuan M (2007) SB401, a pollen-specific protein from *Solanum berthaultii*, binds to and bundles microtubules and F-actin. Plant J 51:406–418

Hussey PJ, Ketelaar T, Deeks MJ (2006) Control of the actin cytoskeleton in plant cell growth. Annu Rev Plant Biol 57:109–125

Ketelaar T, Emons AMC (2001) The cytoskeleton in plant cell growth: lessons from root hairs. New Phytol 152:409–418

Li Y, Shen Y, Cai C, Zhong C, Zhu L, Yuan M, Ren H (2010) The type II *Arabidopsis* formin14 interacts with microtubules and microfilaments to regulate cell division. Plant Cell 22:2710–2726

Liu BQ, Jin L, Zhu L, Li J, Huang S, Yuan M (2009) Phosphorylation of microtubule-associated protein SB401 from *Solanum berthaultii* regulates its effect on microtubules. J Integr Plant Biol 51:235–242

Mineyuki Y, Palevitz BA (1990) Relationship between preprophase band organization, F-actin and the division site in *Allium*. J Cell Sci 97:283–295

Okada S, Fujisawa M, Sone T, Nakayama S, Nishiyama R, Takenaka M, Yamaoka S, Sakaida M, Kono K, Takahama M, Yamato KT, Fukuzawa H, Brennicke A, Ohyama K (2000) Construction of male and female PAC genomic libraries suitable for identification of Y-chromosome-specific clones from the liverwort, *Marchantia polymorpha*. Plant J 24:421–428

Otsu N (1979) A threshold selection method from gray-level histograms. IEEE Trans on Syst Man Cybem 9:62–66

Petrásek J, Schwarzerová K (2009) Actin and microtubule cytoskeleton interactions. Curr Opin Plant Biol 12:728–734

Preuss ML, Kovar DR, Lee YR, Staiger CJ, Delmer DP, Liu B (2004) A plant-specific kinesin binds to actin microfilaments and interacts with cortical microtubules in cotton fibers. Plant Physiol 136:3945–3955

Riedl J, Crevenna AH, Kessenbrock K, Yu JH, Neukirchen D, Bista M, Bradke F, Jenne D, Holak TA, Werb Z, Sixt M, Wedlich-Soldner R (2008) Lifeact: a versatile marker to visualize F-actin. Nat Methods 5:605–607

Seagull RW (1990) The effects of microtubule and microfilament disrupting agents on cytoskeletal arrays and wall deposition in developing cotton fbers. Protoplasma 159:44–59

Sheahan MB, Staiger CJ, Rose RJ, McCurdy DW (2004) A green fluorescent protein fusion to actin-binding domain 2 of *Arabidopsis* fimbrin highlights new features of a dynamic actin cytoskeleton in live plant cells. Plant Physiol 136:3968–3978

Staiger CJ, Cande WZ (1991) Microfilament distribution in *Maize* meiotic mutants correlates with microtubule organization. Plant Cell 3:637–644

Takenaka M, Yamaoka S, Hanajiri T, Shimizu-Ueda Y, Yamato KT, Fukuzawa H, Ohyama K (2000) Direct transformation and plant regeneration of the haploid liverwort *Marchantia polymorpha* L. Transgenic Res 9:179–185

Tominaga M, Morita K, Sonobe S, Yokota E, Shimmen T (1997) Microtubules regulate the organization of actin filaments at the cortical region in root hair cells of *Hydrocharis*. Protoplasma 199:83–92

Tominaga M, Yokota E, Sonobe S, Shimmen T (2000) Mechanism of inhibition of cytoplasmic streaming by a myosin inhibitor, 2,3-butanedione monoxime. Protoplasma 213:46–54

Ueda H, Yokota E, Kutsuna N, Shimada T, Tamura K, Shimmen T, Hasezawa S, Dolja VV, Hara-Nishimura I (2010) Myosin-dependent endoplasmic reticulum motility and F-actin organization in plant cells. Proc Natl Acad Sci USA 107:6894–6899

Van Damme D, Bouget FY, Van Poucke K, Inzé D, Geelen D (2004) Molecular dissection of plant cytokinesis and phragmoplast structure: a survey of GFP-tagged proteins. Plant J 40:386–398

Vidali L, Rounds CM, Hepler PK, Bezanilla M (2009) Lifeact-mEGFP reveals a dynamic apical F-actin network in tip growing plant cells. PLoS ONE 4:e5744

Xu T, Qu Z, Yang X, Qin X, Xiong J, Wang Y, Ren D, Liu G (2009) A cotton kinesin GhKCH2 interacts with both microtubules and microfilaments. Biochem J 421:171–180